Int. J. Solids Structures Vol. 30, No. 13, pp. 1745–1759, 1993
Printed in Great Britain

0020–7683/93 $6.00+ .00

AXISYMMETRIC PROBLEMS OF A PARTIALLY EMBEDDED ROD WITH RADIAL DEFORMATION

RONALD Y. S. PAK and ALAIN T. GOBERT
Department of Civil, Environmental & Architectural Engineering, University of Colorado, Boulder, CO 80309-0428, U.S.A.

(*Received* 6 *July* 1992; *in revised form* 26 *January* 1993)

Abstract—A new mathematical formulation is presented for the analysis of a partially embedded rod under torsionless axisymmetric loadings. With an account of both the axial and radial compatibilities between the rod and the embedding medium through the use of a higher-order rod theory, the three-dimensional load-transfer problem is reduced to a pair of Fredholm integral equations of the second kind whose solutions are computed. By virtue of the present formulation, a variety of physical loading-boundary conditions which were inhibited in past treatments can be evaluated. A comprehensive set of numerical results appropriate to different axial loading conditions, material parameters, and geometric configurations for the problem are provided as illustrations.

1. INTRODUCTION

The response of a partially embedded rod of finite length in an elastic half-space under external loads is a subject of considerable interest in the field of applied mechanics. In material and aerospace engineering, this type of investigation is relevant to the study of fibre-reinforced composites for which the load-transfer process between the matrix and its embedments is important (McCartney, 1989). In civil engineering, such problems are directly related to the soil-structure interaction analysis of piles and anchors commonly employed in foundation design and construction practice (Scott, 1981). For this class of three-dimensional problems in the theory of elasticity, rigorous attempts have thus far been limited. On the axisymmetric problems of axial loading and torsion, the works by Luk and Keer (1979) and Luco (1976) are some of the noteworthy contributions. In these studies, the embedded rods are assumed to be rigid. As a consequence, the influence of the deformability of the embedment on its mechanical interaction with the surrounding medium has not been addressed. The general need to account for the foregoing aspect in practical problems, however, is illustrated in the exact treatment by Muki and Sternberg (1969) on an axially-loaded infinite rod immersed in, and fully bonded to, an infinite medium. Of greater interest, though, is their subsequent contribution to the more difficult problem of axial load diffusion from a partially embedded rod to a semi-infinite solid. With reference to a pilot study contained in their preceding treatment, Muki and Sternberg (1970) employ an approximative scheme in which the embedding medium is extended throughout the half-space and a finite one-dimensional elastic continuum governed by the elementary rod theory is introduced into the region to represent the effects of the embedment. By equating the average axial strain fields of the two media over the common domain, the load-transfer problem is reduced to a Fredholm integral equation of the second kind. Along a similar analytical framework, the problem of a partially embedded bar under lateral loads and moments has likewise been considered (Pak, 1989). With the adoption of the classical beam theory for the embedment, it is shown that the asymmetric load-transfer problem is also amenable to analytical treatment.

The mathematical appeal and practical usefulness of elementary structural theories in numerous engineering applications notwithstanding, their incorporation into this class of structure-continuum interaction problems unfortunately can lead to some fundamental defects. For the finite-rod problem of interest to Muki and Sternberg (1970) for instance, both the axial and radial displacements of the embedment will generally be dependent on the tangential as well as lateral boundary forces exerted on it by the surrounding solid.

With the elementary rod theory which can only address axial deformation due to longitudinal loads, however, one is inherently inhibited from observing proper lateral displacement and traction compatibilities between the two interacting media. Besides running the risk of being unphysical, such an approximation can pose severe limitations on the relevance of the analysis to such important issues as the induced radial stress distribution and the influence of Poisson's effects on the system response.

To address these concerns, it is evident that a more comprehensive treatment for this class of problems is necessary. The purpose of this communication is to introduce such an entry for the examination of the torsionless axisymmetric response of a finite embedded rod whose length of significant load-transfer is suitably large compared to its lateral dimension. In the framework of classical elastostatics and a theory of rods which can accommodate radial deformation, a mathematical formulation for the analysis is developed which is capable of accounting for (i) the deformability of the embedded rod in both the axial and radial directions, (ii) the vectorial effects of contact and kinematic interaction between the rod and the medium, (iii) the Poisson's ratio mismatch of the two media, and (iv) more general boundary and loading conditions at the terminal cross-sections of the embedment. As will be shown in the ensuing derivation, the three-dimensional load-transfer problem can be reduced to a pair of Fredholm integral equations whose solution can be computed. To facilitate direct engineering applications, a set of numerical results appropriate to a number of practical loading conditions, material parameters, and geometric configurations are included as illustrations.

2. MATHEMATICAL FORMULATION

In a circular cylindrical coordinate system (r, θ, z) whose unit base vectors are denoted by $\{\mathbf{e}_r, \mathbf{e}_\theta, \mathbf{e}_z\}$, one considers a cylinderical rod B of length L and radius a partially embedded in a semi-infinite medium S which has a traction-free planar surface (see Fig. 1). For reference, the open cross-sectional region of the rod is denoted by Π; the open half-space is defined by $H = \{x \mid z > 0\}$; the cylindrical subdomain of H occupied by the rod is designated by $D = \{x \mid (r, \theta) \in \Pi,\ 0 < z < L\}$; and the open cross-section of D at $z = s$ is labelled as $\Pi_s = \{x \mid (r, \theta) \in \Pi,\ z = s\}$. Apart from the stated immediate objectives, a primary goal of the present treatment is to establish a basic framework for the general analysis of the load-transfer characteristics of a cylindrical embedment whose stiffness is suitably high compared to that of its surrounding solid, and whose radius is relatively small compared to its length of embedment. To focus on the fundamental aspects of the spatial load-transfer problems of interest, the rod and the embedding medium are assumed to be composed of homogeneous, isotropic, linearly elastic materials for simplicity in this exposition.

For the axisymmetric problems under consideration, the response of the rod-medium system can be fully described by the axial and radial displacement fields, both of which are independent of θ. To render the analysis of the mechanical load diffusion more tractable,

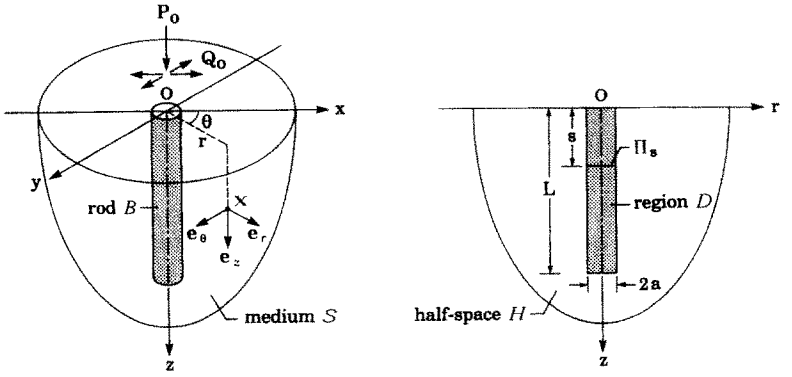

Fig. 1. A partially embedded rod in a half-space.

the embedding medium is extended throughout the half-space H and a fictitious continuum B_* is introduced to D such that the mechanical behavior of the cylindrical region is *equivalent* to that of the actual embedment (Muki and Sternberg, 1970). Appropriate to the class of problems of interest, the extended medium S_* will be regarded as a three-dimensional body within the framework of classical elastostatics. In contrast, the continuum B_* will be treated as a linear elastic rod in the context of a suitable structural mechanics theory. To provide a practical mechanism to deal with the complicated interaction between the two media, however, the development of a simple and yet rational theory which can provide a systematic account of the distributed longitudinal and lateral loads and their relationships to the axial and radial displacements of the rod B_* is needed. For the construction of the desired framework, the use of the principle of minimum potential energy and the calculus of variations is perhaps the most convenient. To this end, it is useful to recognize that the primary deformation mode for an axially-loaded embedded rod of sufficient slenderness and stiffness is axial compression and translation in the longitudinal direction. With this observation in mind, it thus seems logical to represent the axial displacement field w^* of the rod, in a first approximation, as a function of z only. In an axial compression of a rod, however, it should also be evident that there would generally be a corresponding radial displacement field u^* due to Poisson's effect. Moreover, because of its lateral confinement by the surrounding matrix, the cylindrical embedment is likely to experience significant internal radial compression as a result of the load-induced boundary lateral pressure acting on its circumferential surface. As a rudimentary attempt to capture these physical aspects without incurring undue complications, the first nontrivial approximation of the radial variation of u^* over the cross section Π_z as linear is adopted. In addition to their physical relevance and analytical appeal as mentioned above, these kinematic assumptions have proved to be capable of modeling the phenomenon of radial shear which has been found to be important in wave propagation problems (Mindlin and Herrmann, 1951). Taking

$$w^*(r, z) = w_*(z), \quad u^*(z, r) = \left(\frac{r}{a}\right)u_*(z), \tag{1}$$

one is thus led to write the total potential energy of the rod under deformation as

$$\Psi = \int_0^L \left\{ \begin{array}{l} \frac{1}{2}(\lambda_*+2\mu_*)\left(\frac{dw_*}{dz}\right)^2 + 2(\lambda_*+\mu_*)\left(\frac{u_*}{a}\right)^2 \\ \quad +2\lambda_*\left(\frac{u_*}{a}\right)\left(\frac{dw_*}{dz}\right) + \frac{\mu_* J}{2Aa^2}\left(\frac{du_*}{dz}\right)^2 \end{array} \right\} A\,dz$$

$$+\int_0^L \{q_*(z)w_*(z)+t_*(z)u_*(z)\}\,dz$$

$$-P_*(0)w_*(0)+P_*(L)w_*(L)-Q_*(0)u_*(0)+Q_*(L)u_*(L). \tag{2}$$

With reference to the notations and sign convention in Fig. 2, q_* and t_* denote the lineal

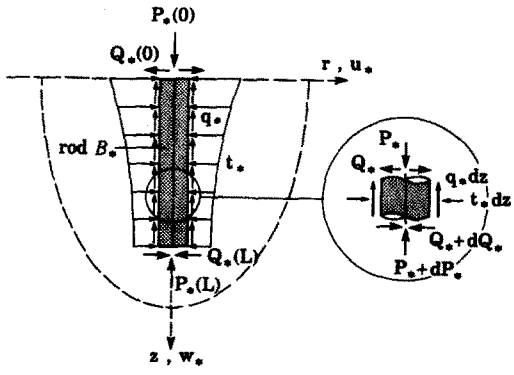

Fig. 2. Axisymmetric loads on the rod B_*.

densities of the distributed longitudinal and radial bond forces acting on B_*; P_* and Q_* are the cross-sectional axial force and radial shear defined by

$$P_*(z) = -\int_{\Pi_z} \sigma_{zz}^* \, dA, \tag{3}$$

$$Q_*(z) = -\int_{\Pi_z} \sigma_{zr}^*\left(\frac{r}{a}\right) dA, \tag{4}$$

where σ_{zz}^* and σ_{zr}^* are the components of the Cauchy stress tensor; λ_*, μ_*, A and J stand for the two Lamé's constants, the cross-sectional area, and the corresponding polar moment of inertia of the rod, respectively. To ensure that the mechanical behavior of the composite region D resembles that of the actual embedment under the foregoing loadings, B_* is to be characterized by

$$\mu_* = \mu_e - \mu_s > 0, \tag{5}$$

$$\lambda_* = \lambda_e - \lambda_s > 0, \tag{6}$$

where the subscripts e and s denote the corresponding quantities of the embedment and of the surrounding solid, respectively.

From the first variation of Ψ with respect to both u_* and w_*, one finds that the two Euler's equations of equilibrium for the rod are

$$(\lambda_* + 2\mu_*)A\frac{d^2 w_*}{dz^2} + \left(\frac{2\lambda_* A}{a}\right)\frac{du_*}{dz} = q_*, \tag{7}$$

$$\left(\frac{\mu_* J}{a^2}\right)\frac{d^2 u_*}{dz^2} - \frac{4(\lambda_* + \mu_*)A}{a^2}u_* - \left(\frac{2\lambda_* A}{a}\right)\frac{dw_*}{dz} = t_*. \tag{8}$$

In the axial direction, the relevant boundary conditions for the present problem are

$$-(\lambda_* + 2\mu_*)A\frac{dw_*}{dz} - 2\lambda_* A\left(\frac{u_*}{a}\right) = P_*(0) \tag{9a}$$

or

$$w_*(0) = w_0 \tag{9b}$$

at $z = 0$ and

$$-(\lambda_* + 2\mu_*)A\frac{dw_*}{dz} - 2\lambda_* A\left(\frac{u_*}{a}\right) = P_*(L) \tag{10}$$

at $z = L$. In the radial direction, the boundary conditions of interest are

$$-\left(\frac{\mu_* J}{a^2}\right)\frac{du_*}{dz} = Q_*(0) \tag{11a}$$

or

$$u_*(0) = u_0 \tag{11b}$$

at $z = 0$ and

$$-\left(\frac{\mu_* J}{a^2}\right)\frac{du_*}{dz} = Q_*(L) \tag{12}$$

at $z = L$. With different combinations of the equations in (9) and (11), there is a variety of physical loading and boundary conditions on the rod that can be investigated. As will be illustrated later, however, there is no loss of generality to consider the load-transfer problem associated with natural boundary conditions only. To this end, consider the response of a partially embedded rod whose unembedded terminal cross-section is subjected to an axial load P_0 and a radial shear Q_0. As can be anticipated, the embedment B_* will generally see nonzero values for the distributed bond-forces t_* and q_* acting along its length, as well as terminal loads in the form of $P_*(0)$, $P_*(L)$, $Q_*(0)$ and $Q_*(L)$. To satisfy equilibrium in both media under the external loadings, the extended medium must therefore receive the opposite reactions of the distributed bond-forces t_* and q_* acting in D, in addition to concentrated load-transfers of $P_0 - P_*(0)$ and $Q_0 - Q_*(0)$ at Π_0 and the terminal load-transfer of $P_*(L)$ and $Q_*(L)$ at Π_L. Issues related to the possible presence of concentrated load-transfers as a result of structure-continuum formulations have been discussed elsewhere (Muki and Sternberg, 1970; Pak, 1989) and will not be repeated here for brevity. In the context of the present formulation, the response of the extended medium to the foregoing loads can be expressed in terms of a pair of normalized vector influence fields $\hat{\mathbf{u}}^Z(x; s) = (\hat{u}_r^Z, 0, \hat{u}_z^Z)$ and $\hat{\mathbf{u}}^R(x; s) = (\hat{u}_r^R, 0, \hat{u}_z^R)$ which are defined as the displacement fields at a point $x \in S_*$ due to suitably distributed axisymmetric internal force fields on Π_s acting in the positive z- and r-directions, respectively. For the convenience of usage, the normalization of $\hat{\mathbf{u}}^Z(x; s)$ is done in accordance with (3) while the one for $\hat{\mathbf{u}}^R(x; s)$ is performed in the sense of (4). To be consistent with the kinematic assumptions of (1) on the cross-sectional deformation of the rod, the source field that yields a uniform u_z over Π and the one that gives a linear variation of u_r over the same region in the interior of an infinite elastic medium are adopted. With the aid of the foregoing influence fields, the displacement of the half-space can be written as

$$\mathbf{u}(x) = [P_0 - P_*(0)]\hat{\mathbf{u}}^Z(x; 0) + P_*(L)\hat{\mathbf{u}}^Z(x; L) + [Q_0 - Q_*(0)]\hat{\mathbf{u}}^R(x; 0) + Q_*(L)\hat{\mathbf{u}}^R(x; L) + \int_0^L q_*(s)\hat{\mathbf{u}}^Z(x; s)\,ds + \int_0^L t_*(s)\hat{\mathbf{u}}^R(x; s)\,ds, \quad x \in S_*. \tag{13}$$

To ensure that the axial and radial deformations of B_* are suitably compatible with that of S_* over the common domain D, the imposition of a set of bond conditions is necessary. For its intuitive and physical appeal, the following set of requirements is enforced over the length of the embedment: (i) the average of the axial displacement u_z of the half-space over Π_z be equal to that of the rod, and (ii) the average of the radial displacement variation u_r/r be equal between the two media. These two bond conditions can be expressed as

$$w_* = \frac{1}{A}\int_{\Pi_z} u_z\,dA, \quad 0 \leqslant z \leqslant L, \tag{14}$$

$$\frac{u_*}{a} = \frac{1}{A}\int_{\Pi_z} \frac{u_r}{r}\,dA, \quad 0 \leqslant z \leqslant L. \tag{15}$$

With the aid of (13), the foregoing equations translate to

$$w_*(z) = [P_0 - P_*(0)]\hat{U}_z^Z(z; 0) + P_*(L)\hat{U}_z^Z(z; L) + [Q_0 - Q_*(0)]\hat{U}_z^R(z; 0) + Q_*(L)\hat{U}_z^R(z; L) + \int_0^L q_*(s)\hat{U}_z^Z(z; s)\,ds + \int_0^L t_*(s)\hat{U}_z^R(z; s)\,ds, \quad 0 \leqslant z \leqslant L, \tag{16}$$

$$\frac{u_*(z)}{a} = [P_0 - P_*(0)]\hat{U}_r^Z(z;0) + P_*(L)\hat{U}_r^Z(z;L)$$
$$+ [Q_0 - Q_*(0)]\hat{U}_r^R(z;0) + Q_*(L)\hat{U}_r^R(z;L)$$
$$+ \int_0^L q_*(s)\hat{U}_r^Z(z;s)\,\mathrm{d}s + \int_0^L t_*(s)\hat{U}_r^R(z;s)\,\mathrm{d}s, \quad 0 \leqslant z \leqslant L, \tag{17}$$

where

$$\hat{U}_z^Z(z;s) = \frac{2}{a^2}\int_0^a \hat{u}_z^Z(z,r;s)r\,\mathrm{d}r, \tag{18}$$

$$\hat{U}_z^R(z;s) = \frac{2}{a^2}\int_0^a \hat{u}_z^R(z,r;s)r\,\mathrm{d}r, \tag{19}$$

$$\hat{U}_r^Z(z;s) = \frac{2}{a^2}\int_0^a \hat{u}_r^Z(z,r;s)r\,\mathrm{d}r, \tag{20}$$

$$\hat{U}_r^R(z;s) = \frac{2}{a^2}\int_0^a \hat{u}_r^R(z,r;s)r\,\mathrm{d}r. \tag{21}$$

3. GOVERNING FREDHOLM INTEGRAL EQUATIONS

For further reduction of the governing equations, it is useful to note that

$$\int_0^L q_*(s)\hat{U}(z;s)\,\mathrm{d}s = (\lambda_* + 2\mu_*)A\int_0^L \frac{\mathrm{d}^2 w_*(s)}{\mathrm{d}s^2}\hat{U}(z;s)\,\mathrm{d}s + \frac{2\lambda_* A}{a}\int_0^L \frac{\mathrm{d}u_*(s)}{\mathrm{d}s}\hat{U}(z;s)\,\mathrm{d}s \tag{22}$$

for an influence field $\hat{U}$. Through an integration by parts with a proper account of the possible discontinuities of the integrands, one finds with the aid of the boundary condition (9a) that (22) gives

$$\int_0^L q_*(s)\hat{U}(z;s)\,\mathrm{d}s = P_*(0)\hat{U}(z;0) - P_*(L)\hat{U}(z;L)$$
$$+ (\lambda_* + 2\mu_*)A\left(-\left[w_*(s)\frac{\partial\hat{U}}{\partial s}(z;s)\right]_0^L + w_*(z)\left[\frac{\partial\hat{U}}{\partial s}(z;s)\right]_{z^-}^{z^+}\right)$$
$$+ (\lambda_* + 2\mu_*)A\int_0^L w_*(s)\frac{\partial^2\hat{U}}{\partial s^2}(z;s)\,\mathrm{d}s - \frac{2\lambda_* A}{a}\int_0^L u_*(s)\frac{\partial\hat{U}}{\partial s}(z;s)\,\mathrm{d}s. \tag{23}$$

Likewise, by virtue of (8) and (11a), one can show that

$$\int_0^L t_*(s)\hat{U}(z;s)\,\mathrm{d}s = Q_*(0)\hat{U}(z;0) - Q_*(L)\hat{U}(z;L) - \frac{2\lambda_* A}{a}([w_*(s)\hat{U}(z;s)]_0^L)$$
$$- \frac{\mu_* J}{a^2}\left(\left[u_*(s)\frac{\partial\hat{U}}{\partial s}(z;s)\right]_0^L - u_*(z)\left[\frac{\partial\hat{U}}{\partial s}(z;s)\right]_{z^-}^{z^+}\right)$$
$$- \frac{4(\lambda_* + \mu_*)A}{a^2}\int_0^L u_*(s)\hat{U}(z;s)\,\mathrm{d}s + \frac{\mu_* J}{a^2}\int_0^L u_*(s)\frac{\partial^2\hat{U}}{\partial s^2}(z;s)\,\mathrm{d}s$$
$$+ \frac{2\lambda_* A}{a}\int_0^L w_*(s)\frac{\partial\hat{U}}{\partial s}\,\mathrm{d}s. \tag{24}$$

Upon application of the foregoing results, the bond conditions (16) and (17) can be reduced to two coupled integral equations on the displacements u_* and w_*. In terms of the dimensionless parameters

$$\bar{z} = \frac{z}{a}, \quad \bar{s} = \frac{s}{a}, \quad \bar{L} = \frac{L}{a}, \quad \bar{u} = \frac{u_*}{a}, \quad \bar{w} = \frac{w_*}{a}, \tag{25}$$

the governing equations for the structure-medium interaction problem can be expressed as

$$A_Z^Z(\bar{z})\bar{w}(\bar{z}) + A_Z^R(\bar{z})\bar{u}(\bar{z}) + B_Z^0(\bar{z})\bar{w}(0) + B_Z^L(\bar{z})\bar{w}(\bar{L}) + C_Z^0(\bar{z})\bar{u}(0) + C_Z^L(\bar{z})\bar{u}(\bar{L}) + \int_0^L K_Z^Z(\bar{z};\bar{s})\bar{w}(\bar{s})\,\mathrm{d}\bar{s} + \int_0^L K_Z^R(\bar{z};\bar{s})\bar{u}(\bar{s})\,\mathrm{d}\bar{s} = F_Z(\bar{z}), \quad 0 \leqslant \bar{z} \leqslant \bar{L}, \tag{26}$$

$$A_R^Z(\bar{z})\bar{w}(\bar{z}) + A_R^R(\bar{z})\bar{u}(\bar{z}) + B_R^0(\bar{z})\bar{w}(0) + B_R^L(\bar{z})\bar{w}(\bar{L}) + C_R^0(\bar{z})\bar{u}(0) + C_R^L(\bar{z})\bar{u}(\bar{L}) + \int_0^L K_R^Z(\bar{z};\bar{s})\bar{w}(\bar{s})\,\mathrm{d}\bar{s} + \int_0^L K_R^R(\bar{z};\bar{s})\bar{u}(\bar{s})\,\mathrm{d}\bar{s} = F_R(\bar{z}), \quad 0 \leqslant \bar{z} \leqslant \bar{L}, \tag{27}$$

where

$$\begin{aligned}
A_Z^Z(\bar{z}) &= \kappa_1\left[\frac{\partial U_z^Z}{\partial \bar{s}}(\bar{z};\bar{s})\right]_{\bar{z}^-}^{\bar{z}^+} - 1,\\
A_Z^R(\bar{z}) &= \kappa_2\left[\frac{\partial U_z^R}{\partial \bar{s}}(\bar{z};\bar{s})\right]_{\bar{z}^-}^{\bar{z}^+},\\
A_R^Z(\bar{z}) &= \kappa_1\left[\frac{\partial U_r^Z}{\partial \bar{s}}(\bar{z};\bar{s})\right]_{\bar{z}^-}^{\bar{z}^+},\\
A_R^R(\bar{z}) &= \kappa_2\left[\frac{\partial U_r^R}{\partial \bar{s}}(\bar{z};\bar{s})\right]_{\bar{z}^-}^{\bar{z}^+} - 1,
\end{aligned} \tag{28}$$

$$\begin{aligned}
B_Z^0(\bar{z}) &= \kappa_1\frac{\partial U_z^Z}{\partial \bar{s}}(\bar{z};0) + \kappa_3 U_z^R(\bar{z};0),\\
B_Z^L(\bar{z}) &= -\kappa_1\frac{\partial U_z^Z}{\partial \bar{s}}(\bar{z};\bar{L}) - \kappa_3 U_z^R(\bar{z};\bar{L}),\\
B_R^0(\bar{z}) &= \kappa_1\frac{\partial U_r^Z}{\partial \bar{s}}(\bar{z};0) + \kappa_3 U_r^R(\bar{z};0),\\
B_R^L(\bar{z}) &= -\kappa_1\frac{\partial U_r^Z}{\partial \bar{s}}(\bar{z};\bar{L}) - \kappa_3 U_r^R(\bar{z};\bar{L}),
\end{aligned} \tag{29}$$

$$\begin{aligned}
C_Z^0(\bar{z}) &= \kappa_2\frac{\partial U_z^R}{\partial \bar{s}}(\bar{z};0),\\
C_Z^L(\bar{z}) &= -\kappa_2\frac{\partial U_z^R}{\partial \bar{s}}(\bar{z};\bar{L}),\\
C_R^0(\bar{z}) &= \kappa_2\frac{\partial U_r^R}{\partial \bar{s}}(\bar{z};0),\\
C_R^L(\bar{z}) &= -\kappa_2\frac{\partial U_r^R}{\partial \bar{s}}(\bar{z};\bar{L}),
\end{aligned} \tag{30}$$

$$K_Z^Z(\bar{z};\bar{s}) = \kappa_1 \frac{\partial^2 U_z^Z}{\partial \bar{s}^2}(\bar{z};\bar{s}) + \kappa_3 \frac{\partial U_z^R}{\partial \bar{s}}(\bar{z};\bar{s}),$$

$$K_Z^R(\bar{z};\bar{s}) = \kappa_2 \frac{\partial^2 U_z^R}{\partial \bar{s}^2}(\bar{z};\bar{s}) - \kappa_3 \frac{\partial U_z^Z}{\partial \bar{s}}(\bar{z};\bar{s}) - \kappa_4 U_z^R(\bar{z};\bar{s}),$$

$$K_R^Z(\bar{z};\bar{s}) = \kappa_1 \frac{\partial^2 U_r^Z}{\partial \bar{s}^2}(\bar{z};\bar{s}) + \kappa_3 \frac{\partial U_r^R}{\partial \bar{s}}(\bar{z};\bar{s}),$$

$$K_R^R(\bar{z};\bar{s}) = \kappa_2 \frac{\partial^2 U_r^R}{\partial \bar{s}^2}(\bar{z};\bar{s}) - \kappa_3 \frac{\partial U_r^Z}{\partial \bar{s}}(\bar{z};\bar{s}) - \kappa_4 U_r^R(\bar{z};\bar{s}), \tag{31}$$

$$F_Z(\bar{z}) = -\bar{P}_0 U_z^Z(\bar{z};0) - \bar{Q}_0 U_z^R(\bar{z};0),$$
$$F_R(\bar{z}) = -\bar{P}_0 U_r^Z(\bar{z};0) - \bar{Q}_0 U_r^R(\bar{z};0), \tag{32}$$

$$U_z^Z(\bar{z};\bar{s}) = 2\pi\mu_s a \hat{U}_z^Z(z;s), \quad U_z^R(\bar{z};\bar{s}) = 2\pi\mu_s a \hat{U}_z^R(z;s),$$
$$U_r^R(\bar{z};\bar{s}) = 2\pi\mu_s a^2 \hat{U}_r^R(z;s), \quad U_r^Z(\bar{z};\bar{s}) = 2\pi\mu_s a^2 \hat{U}_r^Z(z;s), \tag{33}$$

$$\bar{P}_0 = \frac{P_0}{2\pi\mu_s a^2}, \quad \bar{Q}_0 = \frac{Q_0}{2\pi\mu_s a^2}, \tag{34}$$

$$\kappa_1 = \frac{\lambda_* + 2\mu_*}{2\mu_s}, \quad \kappa_2 = \frac{\mu_*}{4\mu_s}, \quad \kappa_3 = \frac{\lambda_*}{\mu_s}, \quad \kappa_4 = \frac{2(\lambda_* + \mu_*)}{\mu_s}. \tag{35}$$

For the analysis of (26) and (27), any two quantities, one from each of the conjugate pairs $(\bar{P}_0, \bar{w}(0))$ and $(\bar{Q}_0, \bar{u}(0))$, can be regarded as prescribed parameters. With such facilities, different combinations of the end-conditions in (9) and (11) can thus be evaluated by virtually the same method. In general, the solution to the pair of governing Fredholm's integral equations of the second kind yields the axial and radial displacements of the rod, which in turn render the response of the system determinate through (7) to (13).

4. INFLUENCE FIELDS

For the determination of the influence fields $\hat{\mathbf{u}}^Z(x;s)$ and $\hat{\mathbf{u}}^R(x;s)$ in an elastic half-space, it is convenient to employ the method of potentials in the theory of elasticity. For torsionless and rotationally symmetric problems such as those under consideration, the solution of the homogeneous displacement equations of equilibrium for an elastic medium can be represented, without loss of completeness, as

$$\mathbf{u}(r,z) = \mathbf{e}_z \nabla^2 \Phi - \frac{1}{2(1-\nu_s)} \nabla(\mathbf{e}_z \cdot \nabla\Phi), \tag{36}$$

where $\Phi(r,z)$ is a biharmonic function satisfying

$$\nabla^4 \Phi(r,z) = 0, \tag{37}$$

with

$$\nabla^4 = \nabla^2 \nabla^2,$$
$$\nabla^2 = \frac{\partial^2}{\partial r^2} + \frac{1}{r}\frac{\partial}{\partial r} + \frac{\partial^2}{\partial z^2} \tag{38}$$

in cylindrical coordinates (Love, 1944). For the internal-load problems of interest, (37) must be appended by the traction-free condition at $z = 0$ that

$$\hat{\sigma}_{zz}(r, 0) = \hat{\sigma}_{rz}(r, 0) = 0, \quad r \geqslant 0, \tag{39}$$

and the regularity conditions at infinity that

$$\hat{\sigma} \to 0, \quad \sqrt{r^2+z^2} \to \infty. \tag{40}$$

Case A : $\hat{\boldsymbol{u}}^Z(x; s)$

The influence field for the axial load-transfer is defined as the response of the half-space to the distributed body-force field

$$R(r) = \hat{\sigma}^Z_{zz}(r, s^-) - \hat{\sigma}^Z_{zz}(r, s^+) = \left\{ \begin{array}{cc} \dfrac{1}{2\pi a\sqrt{a^2-r^2}}, & r < a \\ 0, & r > a \end{array} \right\} \tag{41}$$

whose resultant is unity. By virtue of (36)–(41) and the conditions that $\hat{u}^Z_r$, $\hat{u}^Z_z$ and $\hat{\sigma}^Z_{zr}$ are continuous throughout the medium, one finds a boundary value problem which can be conveniently solved by the method of Hankel transforms. Being a particular solution of (37), the desired influence field $\hat{\mathbf{u}}^Z(x; s)$ can be shown to admit the following integral representations:

$$\hat{u}^Z_z(r, z; s) = \int_0^\infty \Omega_2(\xi, z; s) \frac{Z(\xi)\xi}{\mu_s} J_0(r\xi)\, \mathrm{d}\xi, \tag{42}$$

$$\hat{u}^Z_r(r, z; s) = -\int_0^\infty \gamma_3(\xi, z; s) \frac{Z(\xi)\xi}{\mu_s} J_1(r\xi)\, \mathrm{d}\xi, \tag{43}$$

where

$$\Omega_2(\xi, z; s) = \frac{1}{8(1-\nu_s)\xi} \left\{ \begin{array}{c} (3-4\nu_s+\xi|z-s|)\, \mathrm{e}^{-\xi|z-s|} + \\ ((5-12\nu_s+8\nu_s^2)+(3-4\nu_s)\xi(z+s)+2\xi^2 zs)\, \mathrm{e}^{-\xi(z+s)} \end{array} \right\},$$

$$\gamma_3(\xi, z; s) = \frac{1}{8(1-\nu_s)\xi} \left\{ \begin{array}{c} -(z-s)\xi\, \mathrm{e}^{-\xi|z-s|} + \\ (4(1-2\nu)(1-\nu)-(3-4\nu_s)\xi(z-s)-2\xi^2 zs)\, \mathrm{e}^{-\xi(z+s)} \end{array} \right\},$$

$$Z(\xi) = \frac{\sin(a\xi)}{2\pi a\xi}, \tag{44}$$

and J_p is the Bessel function of the first kind of order p. An integration of (42) and (43) according to (18) and (20) leads to

$$\hat{U}^Z_z(z; s) = \frac{1}{\pi a\mu_s} \int_0^\infty \Omega_2(\xi, z; s) \frac{\sin(a\xi)}{(a\xi)} J_1(a\xi)\, \mathrm{d}\xi, \tag{45}$$

$$\hat{U}^Z_r(z; s) = \frac{-1}{\pi a^2\mu_s} \int_0^\infty \gamma_3(\xi, z; s) \frac{\sin(a\xi)}{(a\xi)} (1-J_0(\xi a))\, \mathrm{d}\xi. \tag{46}$$

In their dimensionless forms, the requisite influence functions due to the axial load can thus be expressed as

$$U^Z_z(\bar{z}; \bar{s}) = 2\int_0^\infty \Omega_2(\bar{\xi}, \bar{z}; \bar{s}) \frac{\sin(\bar{\xi})}{\bar{\xi}} J_1(\bar{\xi})\, \mathrm{d}\bar{\xi}, \tag{47}$$

$$U_r^Z(\bar{z};\bar{s}) = -2\int_0^\infty \gamma_3(\bar{\xi},\bar{z};\bar{s})\frac{\sin(\bar{\xi})}{\bar{\xi}}(1-J_0(\bar{\xi}))\,d\bar{\xi}. \tag{48}$$

Case B: $\hat{\mathbf{u}}^R(x;s)$

The influence field for the radial load-transfer is defined as the response of the half-space to the distributed internal load

$$P(r) = \hat{\sigma}_{zr}^R(r,s^-) - \hat{\sigma}_{zr}^R(r,s^+) = \left\{\begin{array}{ll} \dfrac{3r}{4\pi a^2\sqrt{a^2-r^2}}, & r<a \\ 0, & r>0 \end{array}\right\} \tag{49}$$

which has a unit resultant according to (4). Subject to (37), (39), (40), (49) as well as the conditions that $\hat{u}_r^R$, $\hat{u}_z^R$ and $\hat{\sigma}_{zz}^R$ are continuous in the medium, one finds that the requisite influence field $\hat{\mathbf{u}}^R(x;s)$ can be expressed as

$$\hat{u}_z^R(r,z;s) = -\int_0^\infty \Omega_1(\xi,z;s)\frac{Y(\xi)\xi}{\mu_s}J_0(r\xi)\,d\xi, \tag{50}$$

$$\hat{u}_r^R(r,z;s) = \int_0^\infty \gamma_1(\xi,z;s)\frac{Y(\xi)\xi}{\mu_s}J_1(r\xi)\,d\xi, \tag{51}$$

where

$$\Omega_1(\xi,z;s) = \frac{1}{8(1-\nu_s)\xi}\left\{\begin{array}{c}\xi(z-s)\,e^{-\xi|z-s|}+ \\ (4(1-2\nu_s)(1-\nu_s)+(3-4\nu_s)\xi(z-s)-2\xi^2zs)\,e^{-\xi(z+s)}\end{array}\right\},$$

$$\gamma_1(\xi,z;s) = \frac{1}{8(1-\nu_s)\xi}\left\{\begin{array}{c}(3-4\nu_s-\xi|z-s|)\,e^{-\xi|z-s|}+ \\ ((5-12\nu_s+8\nu_s^2)-(3-4\nu_s)\xi(z+s)+2\xi^2zs)\,e^{-\xi(z+s)}\end{array}\right\},$$

$$Y(\xi) = \frac{3}{4\pi}\left(\frac{\sin(a\xi)}{(a\xi)^2}-\frac{\cos(a\xi)}{(a\xi)}\right). \tag{52}$$

Accordingly, the definitions of (19) and (21) yield

$$\hat{U}_z^R(z;s) = -\frac{3}{2\pi a\mu_s}\int_0^\infty \Omega_1(\xi,z;s)\left(\frac{\sin(a\xi)}{(a\xi)^2}-\frac{\cos(a\xi)}{(a\xi)}\right)J_1(a\xi)\,d\xi, \tag{53}$$

$$\hat{U}_r^R(z;s) = \frac{3}{2\pi a^2\mu_s}\int_0^\infty \gamma_1(\xi,z;s)\left(\frac{\sin(a\xi)}{(a\xi)^2}-\frac{\cos(a\xi)}{(a\xi)}\right)(1-J_0(a\xi))\,d\xi, \tag{54}$$

respectively. By virtue of (53) and (54), the dimensionless influence functions for radial loads are given by

$$U_z^R(\bar{z};\bar{s}) = -3\int_0^\infty \Omega_1(\bar{\xi},\bar{z};\bar{s})\left(\frac{\sin(\bar{\xi})}{\bar{\xi}^2}-\frac{\cos(\bar{\xi})}{\bar{\xi}}\right)J_1(\bar{\xi})\,d\bar{\xi}, \tag{55}$$

$$U_r^R(\bar{z};\bar{s}) = 3\int_0^\infty \gamma_1(\bar{\xi},\bar{z};\bar{s})\left(\frac{\sin(\bar{\xi})}{\bar{\xi}^2}-\frac{\cos(\bar{\xi})}{\bar{\xi}}\right)(1-J_0(\bar{\xi}))\,d\bar{\xi}. \tag{56}$$

As all the integrals in (47), (48), (55), and (56) can be derived analytically (see Appendix), the influence functions can be evaluated in a straightforward manner. Apart from its mathematical appeal, such a feature renders the numerical solution of the pair of integral

equations an economic process. For further analysis, however, it is relevant to note that the second-order derivatives of U_z^Z, U_r^Z, U_z^R and U_r^R, which constitute the kernels of the integral equations, are all square-root singular at $z = s$. For an accurate solution of the two governing Fredholm integral equations, the resulting singularities of the kernels, while integrable, should be accounted for in the numerical process.

5. NUMERICAL RESULTS

For an effective treatment of the pair of weakly singular integral equations, it is useful to employ a numerical method which can negate the effects of the singularity on the convergence of the solution. To this end, the method of singularity subtraction together with a closed N-point Clenshaw–Curtis scheme (1960) is found to be most effective. For a rod of $\bar{L} = 20$ for instance, accurate results can be obtained with $N = 60$. By virtue of the present formulation, a variety of loading and boundary conditions for the axisymmetric load-transfer problem can be investigated. For instance, one may consider the axial compression or extension of an embedded rod whose upper end is either fixed or free radially. One can also examine the response of the rod to an applied radial shear load on its crown which is either fixed or free in the longitudinal direction. In view of their prevalent practical interests and the need of brevity, only the solutions associated with axial loading will be presented. In what follows, the material characterization of the rod-medium system will be given in terms of the shear modulus ratio $\bar{\mu} = \mu_e/\mu_s$ and the Poisson's ratios ν_e and ν_s.

By setting $\bar{Q}_0 = 0$ and $\bar{P}_0 = 1$, one can determine the response of a *smooth-ended* rod per unit axial load via the integral equations (26) and (27). Typical axial displacement profiles of the rod for different modulus ratios are shown in Fig. 3 where all solutions are found to exhibit smooth variations. As the modulus of the rod increases, one can see that the axial displacement would gradually approach a constant, signifying that the rod can eventually be regarded as rigid. The specific value of $\bar{\mu}$ for such a delineation, however, depends on the length of the embedment and the Poisson's ratios of the two media. For the lateral response, it is evident from Fig. 4 that the variation is most significant at the top region. Despite its limited magnitude, the radial displacement is found to be quite sensitive to the values of ν_e and ν_s, with the possibility of having $\bar{u}$ positive or negative depending on the particular circumstances. At the bottom of the embedment, however, a localized radial expansion apparently persists in all cases due to the terminal load-transfer and stress concentrations.

In many engineering applications, the quantity of particular interest is the relationship between the top response of the rod and the applied loads. For the axial-load problem under consideration, the axial compliance function defined by

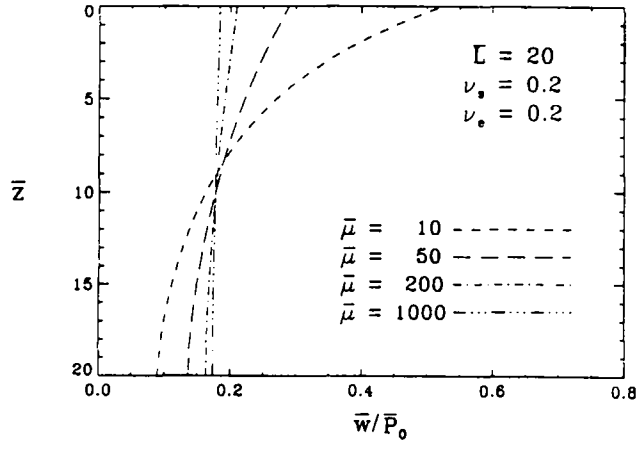

Fig. 3. Axial displacement of a smooth-ended rod.

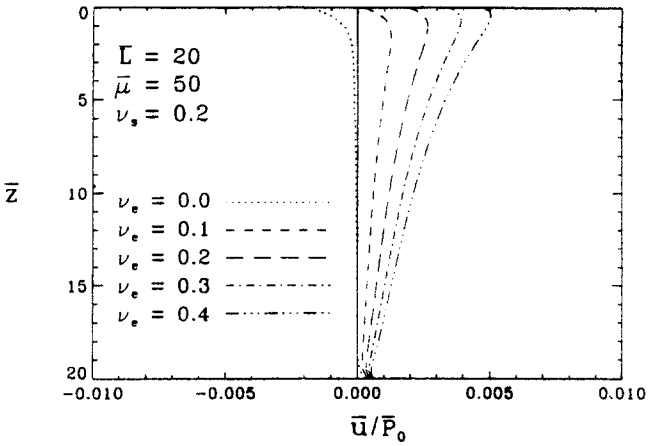

Fig. 4. Radial displacement of a smooth-ended rod.

$$C_{AA} = \frac{\bar{w}(0)}{\bar{P}_0} \tag{57}$$

is perhaps the most important. To this end, its variations with a wide range of $\bar{\mu}$, $\bar{L}$, ν_s, and ν_e are presented in Figs 5 and 6. As can be seen from the result, all four parameters can

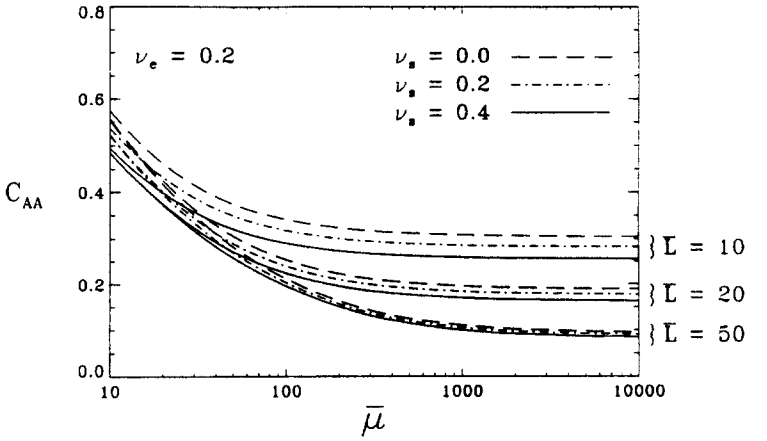

Fig. 5. Axial compliance of a smooth-ended rod as a function of $\bar{\mu}$, $\bar{L}$ and ν_s.

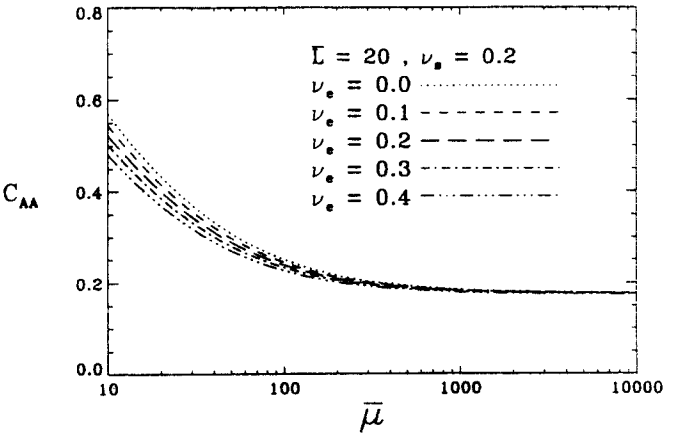

Fig. 6. Influence of ν_e on axial compliance of a smooth-ended rod.

exert a major influence on the axial response. Of immediate practical significance is the confirmation of the existence of a limiting length beyond which further increase in embedment will not result in further reduction of the compliance. From the illustration, one can also observe that the function has a lower bound which depends on the length of the embedment and the Poisson's ratio of the medium, but is independent of the Poisson's ratio of the rod. On the occasion that both the length and stiffness of the rod tend to infinity, one could further deduce from the figures that the influence of both ν_s and ν_e on the axial response would disappear. This is consistent with the observation that the problem would closely resemble one of pure shear in such a limit. At the other end of the picture, one may also notice the coalescence of the solutions for different lengths as $\bar{\mu} \to 1$. Such a trend is, however, in full accord with physical intuition and well supported by a direct consideration of equations (7), (8), (16) and (17) in such a degenerate circumstance.

To assess the influence of boundary conditions on the load-transfer problem, the solution pertaining to a rod whose upper end is subject to the constraint $\bar{u}(0) = 0$, henceforth referred to as the *rough-end* case, is also evaluated. As far as the axial displacement is concerned, such a solution is found to be almost identical to its corresponding smooth-end result along the full length for the static problem under consideration. The comparison of the two radial responses, on the other hand, is more instructive. As an illustration, the rough-end counterpart of Fig. 4 is given in Fig. 7. From the comparison of the displacement profiles, the anticipated departure of the two solutions at the top end of the rod is transparent. Nevertheless, the corresponding pairs of responses do converge rapidly to the same curve as $\bar{z}$ increases which is in tune with Saint-Venant's principle. A revelation of greater importance though is the amount of radial end-shear that can be induced due to the fixity condition. To illustrate the significance of the problem, the ratio of the induced end-shear $\bar{Q}_0$ to the applied axial load $\bar{P}_0$ for the foregoing rod-medium configuration is plotted in Fig. 8. From the display, it is clear that the shear load can easily be of the order of 20–30% of the axial load in either radial directions depending on the relative compressibility of the two media. The fact that there exist finite asymptotic limits for $\bar{Q}_0/\bar{P}_0$ as $\bar{\mu} \to \infty$ should also warrant some attention. Such a consequence is, however, not in conflict with the decays of $\bar{u}(0)$ in Fig. 9 since the end-shear induced by the fixity condition is a function of not only the smooth-end displacement response but also of the shear modulus of the embedment.

6. SUMMARY

In this paper, a new treatment is presented for the analysis of a partially embedded rod under torsionless axisymmetric loadings. With the aid of a theory of rods which can accommodate radial deformation, a mathematical formulation which can provide a rational account of both the axial and radial compatibilities between the two media is established in the form of a pair of Fredholm integral equations of the second kind. Owing to the

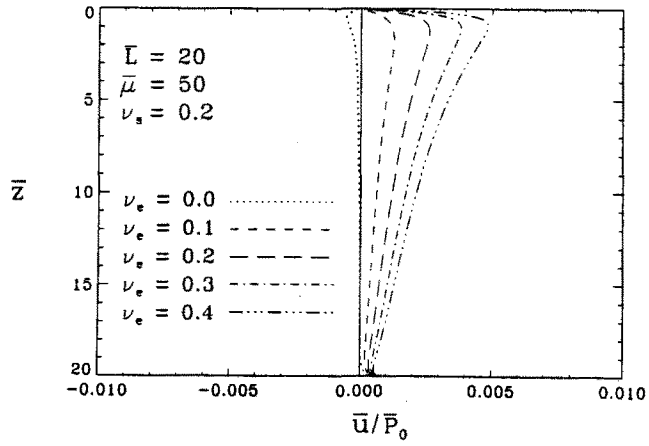

Fig. 7. Radial displacement of a rough-ended rod.

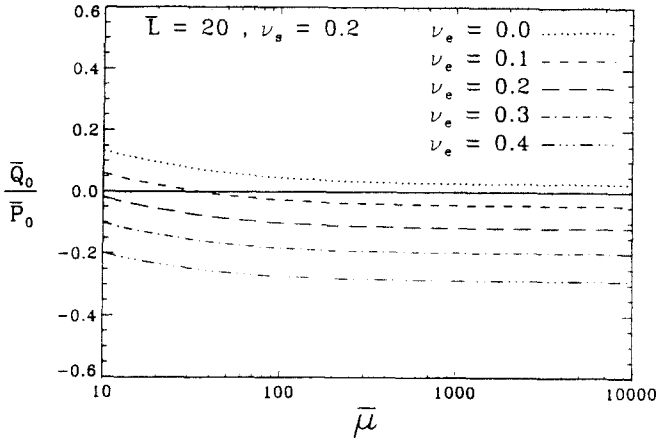

Fig. 8. Top end-shear of a rough-ended rod.

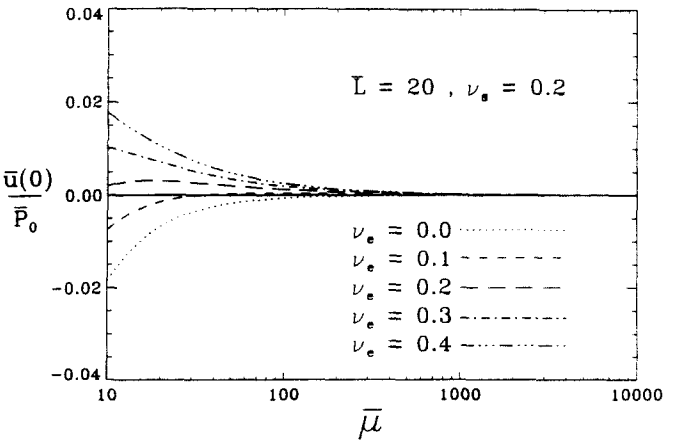

Fig. 9. Top radial displacement of a smooth-ended rod.

generality of the analysis, a variety of physical loading-boundary conditions which were intractable in past treatments can be incorporated. A comprehensive set of numerical results appropriate to different axial loading conditions, material parameters, and geometric configurations for the problem are provided as illustrations. In addition to furnishing information that are pertinent to direct engineering applications, the present treatment should prove useful in providing a consistent framework for a comprehensive analysis of this class of problems.

Acknowledgement—The support provided by the U.S. National Science Foundation through the Presidential Young Investigator Award BCS-8958402 to R. Y. S. P. during the course of this investigation is gratefully acknowledged.

REFERENCES

Clenshaw, C. W. and Curtis, A. R. (1960). A method for numerical integration on an automatic computer. *Numer. Math.* **2**, 197–205.

Love, A. E. K. (1944). *A Treatise on the Mathematical Theory of Elasticity* (4th Edn). Dover, New York.

Luco, J. E. (1976). Torsion of a rigid cylinder embedded in an elastic half-space. *J. Appl. Mech., ASME* **43**, 419–423.

Luk, V. K. and Keer, L. M. (1979). Stress analysis for an elastic half-space containing an axially-loaded rigid cylindrical rod. *Int. J. Solids Structures* **15**, 805–827.

McCartney, L. M. (1989). New theoretical model of stress transfer between fibre and matrix in a uniaxially fibre-reinforced composites. *Proc. R. Soc. Lond.* **A425**, 215–244.

Mindlin, R. D. and Herrmann, G. (1951). A one-dimensional theory of compressional waves in an elastic rod. *Proc. 1st Nat. Congr. Appl. Mech.*, Chicago, pp. 187–191.

Muki, R. and Sternberg, E. (1969). On the diffusion of an axial load from an infinite cylindrical bar embedded in an elastic medium. *Int. J. Solids Structures* **5**, 587–605.

Muki, R. and Sternberg, E. (1970). Elastostatic load-transfer to a half-space from a partially embedded axially loaded rod. *Int. J. Solids Structures* **6**, 69–90.
Pak, R. Y. S. (1989). On the flexure of a partially embedded bar under lateral loads. *J. Appl. Mech., ASME* **56**(2), 263–269.
Scott, R. F. (1981). *Foundation Analysis*. Prentice-Hall, Englewood Cliffs, NJ.

APPENDIX

Notation

$$S(d; n, p) = \int_0^\infty \xi^n e^{-\xi d} \sin(\xi) J_p(\xi)\, d\xi,$$

$$C(d; n, p) = \int_0^\infty \xi^n e^{-\xi d} \cos(\xi) J_p(\xi)\, d\xi,$$

$$S(d; n) = \int_0^\infty \xi^n e^{-\xi d} \sin(\xi)\, d\xi,$$

$$C(d; n) = \int_0^\infty \xi^n e^{-\xi d} \cos(\xi)\, d\xi.$$

$$\alpha = d - i, \quad d > 0.$$

Results

$$S(d; -1) = \tan^{-1}\left(\frac{1}{d}\right),$$

$$S(d; n) = \mathrm{Im}\left(\frac{n!}{(d-i)^{n+1}}\right), \quad n > -1,$$

$$C(d; n) = \mathrm{Re}\left(\frac{n!}{(d-i)^{n+1}}\right), \quad n > -1,$$

$$S(d; -2, 1) = \left[\frac{d\sqrt{d^2+4}+d^2}{2}\right]^{1/2} - \left[\frac{\sqrt{d^2+4}-d}{4}\right]\left[\frac{d\sqrt{d^2+4}-d^2}{2}\right]^{1/2} + \tfrac{1}{2}\sin^{-1}\left[\frac{\sqrt{d^2+4}-d}{2}\right] - d,$$

$$S(d; -1, 1) = \mathrm{Im}[\sqrt{\alpha^2+1} - \alpha],$$

$$C(d; -1, 1) = \mathrm{Re}[\sqrt{\alpha^2+1} - \alpha],$$

$$S(d; 0, 1) = \mathrm{Im}\left[1 - \frac{\alpha}{\sqrt{\alpha^2+1}}\right],$$

$$C(d; 0, 1) = \mathrm{Re}\left[1 - \frac{\alpha}{\sqrt{\alpha^2+1}}\right],$$

$$S(d; 1, 1) = \mathrm{Im}\left[\frac{1}{(1+\alpha^2)^{3/2}}\right],$$

$$C(d; 1, 1) = \mathrm{Re}\left[\frac{1}{(1+\alpha^2)^{3/2}}\right],$$

$$S(d; 2, 1) = \mathrm{Im}\left[\frac{3\alpha}{(1+\alpha^2)^{5/2}}\right],$$

$$C(d; 2, 1) = \mathrm{Re}\left[\frac{3\alpha}{(1+\alpha^2)^{5/2}}\right],$$

$$\int_0^\infty \frac{\sin\xi}{\xi^2} e^{-\xi d}(1 - J_0(\xi))\, d\xi = \sum_{k=0}^{\infty} \frac{(-1)^k}{2^{2k+2}[(k+1)!]^2} S(d; 2k),$$

$$\int_0^\infty \left(\frac{\sin\xi}{\xi^3} - \frac{\cos\xi}{\xi^2}\right) e^{-\xi d}(1 - J_0(\xi))\, d\xi = \sum_{k=0}^{\infty} \frac{(-1)^k}{2^{2k+2}[(k+1)!]^2} [S(d; 2k-1) - C(d; 2k)],$$

$$\int_0^\infty \left(\frac{\sin\xi}{\xi^2} - \frac{\cos\xi}{\xi}\right) e^{-\xi d}(1 - J_0(\xi))\, d\xi = S(d; -1, 1) + S(d; -1, 0) - S(d; -1)d,$$

$$\int_0^\infty \frac{\sin\xi}{\xi^2} e^{-\xi d} J_2(\xi)\, d\xi = \tfrac{1}{2} - S(d; -2, 1)d - \sum_{k=0}^{\infty} \frac{(-1)^k}{2^{2k+2} k!(k+2)!} S(d; 2k).$$